

# Pd site doping effect on superconductivity in $\text{Nb}_2\text{Pd}_{0.76}\text{S}_5$

C. Y. SHEN<sup>1</sup>, B. Q. SI<sup>1</sup>, H. BAI<sup>1</sup>, X. J. YANG<sup>1</sup>, Q. TAO<sup>1</sup>, G. H. CAO<sup>1,2,3</sup> and Z. A. XU<sup>1,2,3</sup>

<sup>1</sup> Department of Physics and State Key Laboratory of Silicon Materials, Zhejiang University, Hangzhou 310027, China

<sup>2</sup> Zhejiang California International NanoSystems Institute, Zhejiang University, Hangzhou 310058, China

<sup>3</sup> Collaborative Innovation Centre of Advanced Microstructures, Nanjing 210093, China

PACS 74.70.Xa – Pnictides and chalcogenides

PACS 74.25.F- – Transport properties of superconductors

PACS 74.62.-c – Transition temperature variations, phase diagrams

**Abstract** – Pd site doping effect on superconductivity was investigated in quasi-one-dimensional superconductor  $\text{Nb}_2(\text{Pd}_{1-x}\text{R}_x)_{0.76}\text{S}_5$  ( $\text{R}=\text{Ir}, \text{Ag}$ ) by measuring resistivity, magnetic susceptibility and Hall effect. It was found that superconducting transition temperature ( $T_c$ ) is firstly slightly enhanced by partial substitution of Pd with Ir and then it is suppressed gradually as Ir content increases further. Meanwhile Ag substitution quickly suppresses the system to a non-superconducting ground state. Hall effect measurements indicate the variations of charge carrier density caused by Ir or Ag doping. The established phase diagram implies that the charge carrier density (or the band filling) could be one of the crucial controlling factors to determine  $T_c$  in this system.

**Introduction.** – Recently superconductivity with  $T_c$  of about 7 K has been discovered in a transition-metal chalcogenide  $\text{Nb}_2\text{PdS}_5$ , which displays extremely large upper critical field ( $H_{c2}$ ), violating the Pauli paramagnetic limit [1] by a factor of 3 [2, 3]. In contrast to the iron pnictides, this compound crystallizes in a lower symmetry space-group  $\text{C2/m}$  and was argued to be a multi-band superconductor [2]. Further investigation on the substitution effect shows that superconductivity is still alive at  $T_c \sim 6$  K by replacing Nb with Ta [4], which is proposed to be close to the Anderson localization state. On the other hand,  $T_c$  is systematically suppressed by partially substituting S by Se and eventually superconductivity disappears with a semiconducting ground state at 50% Se substitution in  $\text{Nb}_2\text{PdS}_{5-x}\text{Se}_x$  [5], but  $T_c$  is still as high as 2.5 K in the Ta-based system  $\text{Ta}_2\text{PdSe}_5$  [6]. The large upper critical field ( $H_{c2}$ ) is confirmed in all these superconductors [2, 4, 6, 7], which implies that it is a universal feature and these quasi-one-dimensional (Q1D) compounds may belong to a new family of unconventional superconductors.

The spin-orbit coupling (SOC) has been speculated to be a potential ingredient for the unconventional properties in these Q1D superconductors. The ratio of  $H_{c2}$  to  $T_c$  was reported to be significantly enhanced by doping Pt into  $\text{Nb}_2\text{PdS}_5$  system due to the strong spin-orbit coupling [8]. This is also consistent with the argument that the

high  $H_{c2}$  of  $\text{Ta}_2\text{PdS}_5$  and  $\text{Nb}_2\text{PdSe}_5$  derives from the large SOC of heavy Pd element [4, 7]. In addition, according to the theoretical study of the electronic structure of these compounds, 4d electrons of Pd contribute to the Fermi surface mostly [2, 7] and thus it is believed that the heavy element Pd with 4d electrons should play a key role in the mechanism of superconductivity [2, 9], but there are very few studies on this issue.

In this Letter, we focus on the doping effect on Pd site by heterovalent transition metals such as Ir and Ag. It turns out that superconductivity can be slightly enhanced by partial substitution of Pd by Ir, but is suppressed rapidly with Ag doping. A phase diagram of  $\text{Nb}_2(\text{Pd}_{1-x}\text{R}_x)_{0.76}\text{S}_5$  ( $\text{R}=\text{Ir}, \text{Ag}$ ) is established, which indicates that superconductivity is systematically affected by the 4d or 5d electron numbers on the Pd site, and the charge carrier density could be one of the crucial factors to control superconductivity in  $\text{Nb}_2\text{Pd}_{0.76}\text{S}_5$ .

**Experiment.** – Poly-crystalline samples of  $\text{Nb}_2\text{Pd}_{1-x}\text{R}_x\text{S}_5$  ( $\text{R}=\text{Ir}, \text{Ag}$ ) were synthesized by a solid-state reaction method. Powders of Nb(99.99%), Pd(99.99%), Ir or Ag (99.99%), and S(99.9%) were mixed and pelletized in a stoichiometric ratio of 2:1- $x$ : $x$ :6. The pellets were then sealed in an evacuated quartz tube followed by a sintering procedure at 1123 K for 24 h. All procedures were performed in a glove box

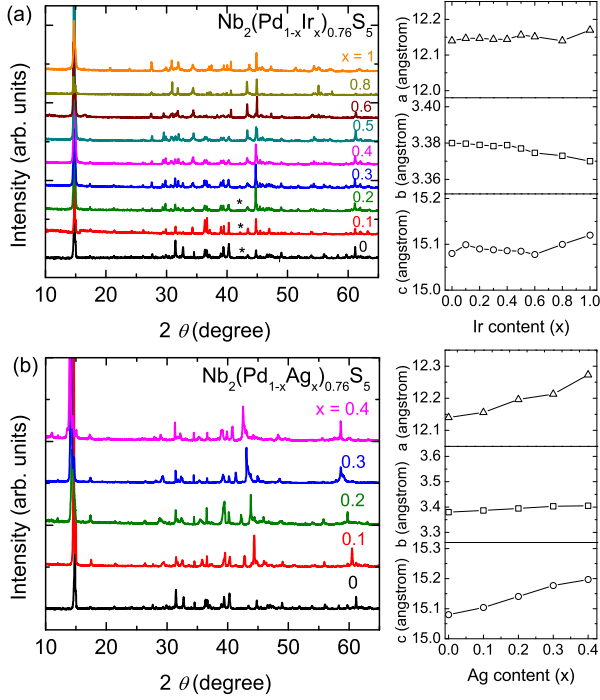


Fig. 1: (a) Powder X-ray diffraction patterns at room temperature for  $\text{Nb}_2(\text{Pd}_{1-x}\text{Ir}_x)_{0.76}\text{S}_5$  with  $x$  from 0 to 1. (b) XRD patterns for  $\text{Nb}_2(\text{Pd}_{1-x}\text{Ag}_x)_{0.76}\text{S}_5$  with  $x = 0, 0.1, 0.2, 0.3$  and  $0.4$  respectively. The right panel plots Ir(Ag) doping dependence of lattice parameters, where  $a$ ,  $b$  and  $c$  are denoted by triangle, square and circle symbols respectively. Minor peaks from impurity are marked by asterisks.

filled with high-purity argon except for the sintering process. The obtained samples usually shows Pd site deficiency, which were found to be around 0.24 according to the measurements of energy-dispersive x-ray spectroscopy (EDX). Namely the samples can be described as  $\text{Nb}_2(\text{Pd}_{1-x}\text{R}_x)_{0.76}\text{S}_5$ . Both area (of about  $4\mu\text{m}^2$ ) and spot scans were used in the EDX measurements and the estimated errors are about 3%-5%.

Room temperature powder X-ray diffraction (XRD) was performed using a PANalytical x-ray diffractometer (Model EMPYREAN) with a monochromatic  $\text{Cu-K}\alpha$  radiation. The electrical resistivity was measured using a standard four-terminal method. The Hall effect was performed on a Quantum Design physical property measurement system (PPMS-9). The DC magnetization measurements were performed on a Quantum Design magnetic property measurement system (MPMS-5). Both the zero field-cooling (ZFC) and field-cooling (FC) measurements were applied.

**RESULTS AND DISCUSSION.** — Figure 1 (a) and (b) show the XRD patterns for the samples of  $\text{Nb}_2(\text{Pd}_{1-x}\text{Ir}_x)_{0.76}\text{S}_5$  and  $\text{Nb}_2(\text{Pd}_{1-x}\text{Ag}_x)_{0.76}\text{S}_5$  respectively. The main XRD peaks can be well indexed based on

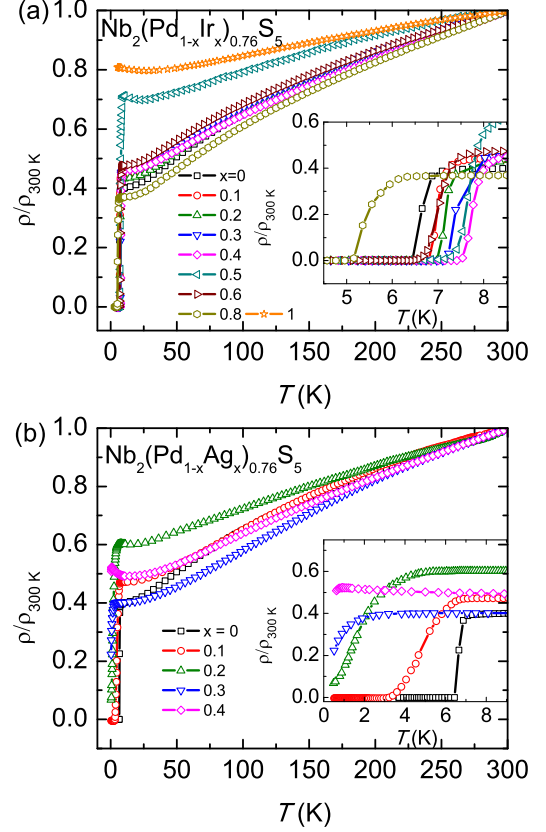


Fig. 2: (a) Temperature dependence of normalized resistivity for  $\text{Nb}_2(\text{Pd}_{1-x}\text{Ir}_x)_{0.76}\text{S}_5$  with  $x$  from 0 to 1. (b) Temperature dependence of normalized resistivity for  $\text{Nb}_2(\text{Pd}_{1-x}\text{Ag}_x)_{0.76}\text{S}_5$  with  $x = 0, 0.1, 0.2, 0.3$  and  $0.4$  respectively. The insets zoom in the low temperature regimes below 8 K.

the C2/m space group except a few minor peaks assigned as impurity phase marked by the asterisks, which is unknown yet. The right panels plot the lattice parameters as a function of nominal Ir or Ag content. It is found that for Ir doping, the lattice parameters seem less dependent on the Ir content due to the comparable ion radius of Ir and Pd. In contrast, the  $a$  and  $c$  axis for the Ag-doped samples increase monotonically, consisting with the large radius of Ag ion, while the  $b$  axis does not change so much.

The temperature dependence of resistivity for  $\text{Nb}_2(\text{Pd}_{1-x}\text{Ir}_x)_{0.76}\text{S}_5$  and  $\text{Nb}_2(\text{Pd}_{1-x}\text{Ag}_x)_{0.76}\text{S}_5$  is presented in fig. 2. Each curve has been normalized by its room temperature value for easy presentation. The absolute values of resistivity at 300 K range from  $1.21\text{ m}\Omega \cdot \text{cm}$  to  $3.09\text{ m}\Omega \cdot \text{cm}$ , comparable with that found in  $\text{Nb}_2\text{Pd}_x\text{Se}_5$  [7]. For the undoped compound  $\text{Nb}_2\text{Pd}_{0.76}\text{S}_5$ ,  $\rho(T)$  remains metallic and becomes superconducting below 6.8 K. Upon doping, a small upturn can be seen in  $\rho(T)$  at low temperatures, which is also found in Ta or Se doped samples due to the proximity to an Anderson localization associated with strong disorders [4, 5]. Such a small upturn in resistivity could also be caused by

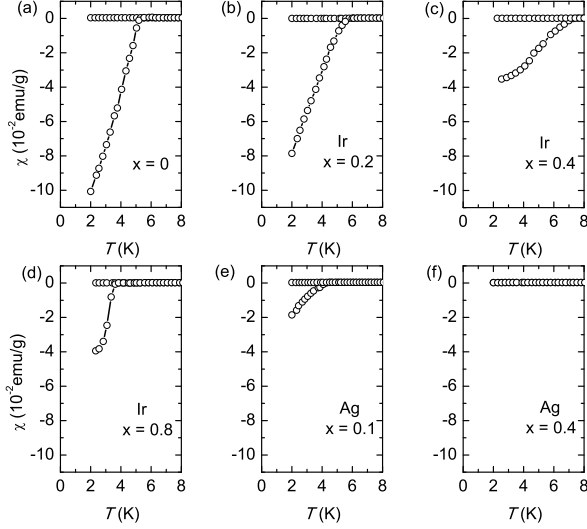


Fig. 3: Temperature dependence of the dc magnetic susceptibility under ZFC and FC protocols for  $\text{Nb}_2(\text{Pd}_{1-x}\text{Ir}_x)_{0.76}\text{S}_5$  and  $\text{Nb}_2(\text{Pd}_{1-x}\text{Ag}_x)_{0.76}\text{S}_5$  samples under a magnetic field of 10 Oe below 8 K.

the grain boundary effect in polycrystalline samples, as reported previously in the high- $T_c$  cuprates [10]. Meanwhile, the critical temperature  $T_c$  starts to increase with Ir doping and reaches a maximum of 8 K at  $x = 0.4$ , then  $T_c$  rapidly decreases and drops below 0.5 K at  $x = 1$ . While for  $\text{Nb}_2(\text{Pd}_{1-x}\text{Ag}_x)_{0.76}\text{S}_5$ , the superconductivity is suppressed quickly with increasing Ag content and finally disappears (for  $T > 0.5\text{K}$ ) with 40% substitution of Ag. The bulk nature of the superconductivity for the doping samples was confirmed by the magnetization measurements, as given in fig. 3, where large diamagnetic signals can be clearly seen for the superconducting samples.

Figure 4 shows the Hall coefficient ( $R_H$ ) as a function of temperature for  $\text{Nb}_2(\text{Pd}_{1-x}\text{Ir}_x)_{0.76}\text{S}_5$  and  $\text{Nb}_2(\text{Pd}_{1-x}\text{Ag}_x)_{0.76}\text{S}_5$  samples respectively. It may be noted that the Hall coefficient is usually not very sensitive to grain boundaries [10, 11]. The  $R_H$  of  $\text{Nb}_2(\text{Pd}_{1-x}\text{Ir}_x)_{0.76}\text{S}_5$  is positive in normal state, suggesting the dominant charge transport by the hole conduction. This positive  $R_H$  confirms the hole doping by substituting Pd with the Ir element. On the other hand, the negative Hall coefficient for  $\text{Nb}_2(\text{Pd}_{1-x}\text{Ag}_x)_{0.76}\text{S}_5$  implies the electron dominant transport properties in the Ag doped samples, which is in agreement with the additional electrons induced by replacing Pd with Ag. The normal state  $R_H(T)$  exhibits very weak temperature dependence, which is usually observed in conventional one-band metals. For a multi-band system, a strong temperature dependence of  $R_H$  is often expected. In addition, the linear magnetic field dependence of the Hall resistivity found in  $\text{Nb}_2\text{Pd}_{1.2}\text{Se}_5$  [7] is also observed in our samples, suggesting that the Hall effect could be dominated by only one type of charge carriers.

The middle point of superconducting transition temper-

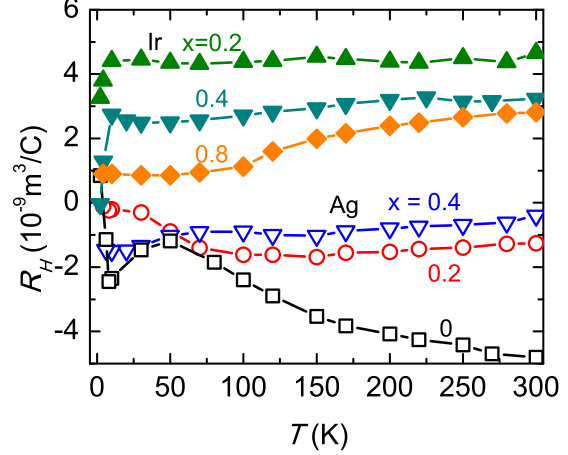


Fig. 4: Temperature dependence of the Hall coefficient for  $\text{Nb}_2(\text{Pd}_{1-x}\text{Ir}_x)_{0.76}\text{S}_5$  (full symbols) and  $\text{Nb}_2(\text{Pd}_{1-x}\text{Ag}_x)_{0.76}\text{S}_5$  samples (empty symbols) respectively.

ature in resistivity,  $T_c^{mid}$ , for  $\text{Nb}_2(\text{Pd}_{1-x}\text{R}_x)_{0.76}\text{S}_5$  ( $\text{R}=\text{Ir}, \text{Ag}$ ) as well as the estimated charge carrier density ( $n$ ) extracted from  $R_H$  at  $T = 150\text{ K}$  and  $300\text{ K}$  is plotted against Ag (Ir) content ( $x$ ) in fig. 5. Since the Hall effect might be dominated by one band, we just simply assume a single band model to estimate the carrier density using  $R_H = \frac{1}{ne}$ . Although the carrier density extracted through a single band model is not very accurate considering the complex Fermi surfaces in this system, it could still give a qualitative estimation on the evolution of carrier numbers with the doping. Giving the heterovalent doping of Ir and Ag, it is believed that such dopants will change the carrier density in the system, which is indeed confirmed by the Hall measurements. As shown in fig. 5, a monotonic increase of the carrier density with increasing Ir (Ag) doping is clearly observed, although the change rate of carrier density with doping content ( $x$ ) for the two dopants are slightly different. Overall, superconductivity is firstly enhanced by the hole-type doping (Ir doping) and  $T_c^{mid}$  reaches the highest value ( $\sim 8\text{ K}$ ) around  $x$  (Ir) = 0.4. But upon further hole doping,  $T_c^{mid}$  is rapidly suppressed. On the contrast, with electron-type doping (Ag doping),  $T_c^{mid}$  decreases monotonically with  $x$  (i.e., increasing electron carrier density), and finally superconductivity disappears (for  $T > 0.5\text{ K}$ ), suggesting a significant negative correlation between electron-type carrier density and superconductivity. Thus our data illustrate that the suitable charge carrier density (or band filling) could be crucial to the occurrence of superconductivity.

The observation above could be understood in the following scenario. According to the band calculations [2, 7], the parent compound  $\text{Nb}_2\text{PdS}_5$  has been predicted to be very close to an itinerant magnetically ordered state with a complex Fermi surface (FS) composed of Quasi-two-dimensional (Q2D) sheets of hole character and strongly warped quasi-one-dimensional sheets of both hole and

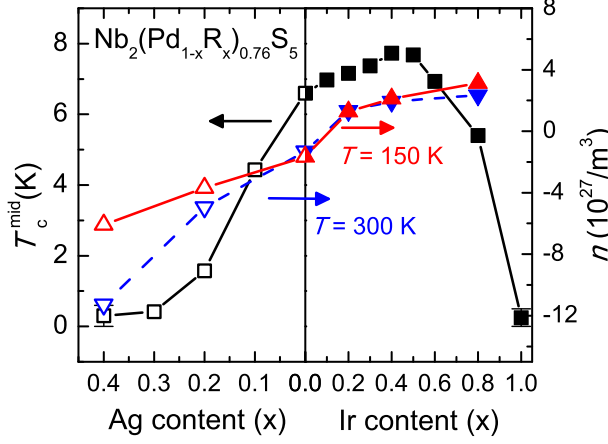


Fig. 5: Phase diagram of  $T_c^{\text{mid}}$  (square),  $n_{T=150\text{K}}$  (upper triangle, solid line) and  $n_{T=300\text{K}}$  (down triangle, dashed line) vs. doping for  $\text{Nb}_2(\text{Pd}_{1-x}\text{Ir}_x)_{0.76}\text{S}_5$  (full symbols) and  $\text{Nb}_2(\text{Pd}_{1-x}\text{Ag}_x)_{0.76}\text{S}_5$  (empty symbols). The negative (positive) value of  $n_{T=150\text{K}}$  (or  $n_{T=300\text{K}}$ ) indicates the electron (hole)-type charge carriers.

electron. By adding a small amount of extra negative (electron) charge into the system, the very flat band near Fermi energy will become the Q1D Fermi surface sheets, giving rise to strong nesting properties as well as large density states, so that the long range magnetic order could be stabilized. It is well known that, in many unconventional superconductors, the magnetic order such as anti-ferromagnetism and spin density wave (SDW) competes with superconductivity [12,13]. Therefore the negative correlation between electron-type charge carrier density and superconductivity in  $\text{Nb}_2\text{Pd}_{0.76}\text{S}_5$  could be well understood in this manner. Namely Ag doping induces electron-type charge carriers to the system and then drives it even close to the magnetic instability. Another possible scenario is that the strong nest properties of FS may allow the formation of charge density wave (CDW) in low-dimensional systems, which usually competes with superconductivity [7]. In this case, Ag doping may drive the system close to the CDW order. Nevertheless, the situation for the hole doping (Ir doping) is somewhat complicated.  $T_c$  initially increase with hole-type charge carrier density, reaches a maximum of about 8 K, then decreases quickly with further hole-type doping. Although we can naively assume that the hole-type doping could drive the system away from the magnetic instability and thus it has a positive effect on superconductivity, the reason why  $T_c$  drops with further Ir doping remains an open issue. Note that the chemical pressure, for example, the substitution of S by Se [5], could reduce  $T_c$  significantly in this Q1D system. However, in the case of Ir-for-Pd doping, the lattice parameters do not change so much, thus the effect of chemical pressure might be ruled out. Another possible explanation may be related to the variation in the strength of the

spin-orbit coupling due to Ir doping. Since Ir has larger atomic number than Pd, its inherent SOC should be naturally larger than that of Pd. Therefore, with increasing Ir doping, the strength of SOC could be enhanced. However, recent experimental studies on superconductivity of the  $\text{LaAlO}_3/\text{SrTiO}_3$  interface and the transport properties in a Pb thin film under an in-plane magnetic field show that large SOC has a positive impact on low-dimensional superconductivity [14,15]. Moreover, a theoretical study on Bi-rich compounds  $\text{ABi}_3$  (A=Sr and Ba) [16], which are of a three-dimensional structure, demonstrates that superconductivity could be significantly enhanced due to the phonon softening and an increase in electron-phonon coupling induced by SOC. Therefore, the effect of SOC on  $T_c$  in  $\text{Nb}_2\text{PdS}_5$  system is an interesting issue. In the case of Pt doping, in contrast to Ir doping,  $T_c$  is depressed, but its SOC should be enhanced [8] as in the Ir-doping case.

An interesting feature of the phase diagram shown in fig. 5 is that the dependence of  $T_c$  on the charge carrier density is also dome-like, which mimics the phase diagram in high- $T_c$  superconductors such as the cuprates [17] and iron pnictides [18] despite of the sign change in the dominant charge carriers. Upon electron (hole) doping, superconductivity emerges and  $T_c$  increases, reaches a maximum at an “optimal doping level” at  $x$  (Ir) = 0.4, and then it is suppressed quickly. Finally superconductivity disappears in the so-called “overdoped region”. Giving that the parents compounds of cuprates and iron pnictides are antiferromagnetically (AFM) ordered [19,20], the proximity to a long range magnetic order in the  $\text{Nb}_2\text{PdS}_5$  system predicated by the band calculations, though not experimentally observed so far, implies the similarity in phase diagrams for these unconventional superconductors, which may imply that the mechanism of superconductivity of the  $\text{Nb}_2\text{PdS}_5$  system could have a close relationship with these systems. On the other hand, superconductivity is often found close to a quantum critical point (QCP) in the materials where a long-range magnetic order is gradually suppressed as a function of a control parameter such as charge-carrier doping or pressure. It is an interesting issue if there exists a parent compound with magnetic order in the  $\text{Nb}_2\text{PdS}_5$  system and a magnetic QCP accompanied by the emergence of superconductivity.  $\text{Nb}_2\text{Pd}_{0.76}\text{S}_5$  is found to be Fermi-liquid like in the temperature range just above  $T_c$ , however, other chalcogenides such as  $\text{Nb}_2\text{Pd}_x\text{Se}_5$  [7] and  $\text{Nb}_3\text{Pd}_x\text{Se}_7$  [9] display metallic state with non-Fermi-liquid behavior at very low temperatures. To elucidate such issues, more theoretical and experimental studies are required.

**CONCLUSION.** – In summary, we have investigated the superconducting properties in the  $\text{Nb}_2(\text{Pd}_{1-x}\text{R}_x)_{0.76}\text{S}_5$  (R=Ir, Ag) polycrystalline samples. It is found that superconductivity can be enhanced by partial substitution of Ir but is quickly suppressed to a nonsuperconducting ground state with 40% Ag doping. Ag doping is an electron-type dopant and Ir doping could



be regarded as the hole-type dopant as suggested by the Hall effect measurements. The overall phase diagram indicates a domelike dependence of  $T_c$  on the doping level, which mimics the general phase diagrams of high- $T_c$  superconducting cuprates and some other unconventional superconductors. Our work implies that there could exist a competing order, either magnetic order or charge order in this system and the charge carrier density (or band filling) is one of the crucial factors to tune the superconducting order.

\* \* \*

The work is supported by the National Basic Research Program of China (Grant Nos. 2014CB921203 and 2012CB821404), the National Science Foundation of China (Grant Nos. 11190023, U1332209 and 11174247), and the Fundamental Research Funds for the Central Universities of China.

## REFERENCES

- [1] CLOGSTON A., *Phys. Rev. Lett.*, **9** (1962) 266.
- [2] ZHANG Q., LI G., RHODES D., KISWANDHI A., BESARA T., ZENG B., SUN J., SIEGRIST T., JOHANNES M. and BALICAS L., *Sci. Rep.*, **3** (2013) 1446.
- [3] YU H.-Y., ZUO M., ZHANG L., TAN S., ZHANG C.-J. and ZHANG Y.-H., *J. Am. Chem. Soc.*, **135** (2013) 12987.
- [4] LU Y.-F., TAKAYAMA T., BANGURA A. F., KATSURA Y., HASHIZUME D. and TAKAGI H., *J. Phys. Soc. Jpn.*, **83** (2013) 023702.
- [5] NIU C.-Q., YANG J.-H., LI Y.-K., CHEN B., ZHOU N., CHEN J., JIANG L.-L., CHEN B., YANG X.-X., CAO C., DAI J.-H. and XU X.-F., *Phys. Rev. B*, **88** (2013) 104507.
- [6] ZHANG J., DONG J.-K., XU Y., PAN J., HE L.-P., ZHANG L.-J. and LI S.-Y., *Supercond. Sci. Technol.*, **28** (2015) 115015.
- [7] KHIM S., LEE B., CHOI K.-Y., JEON B.-G., JANG D. H., PATIL D., PATIL S., KIM R., CHOI E. S., LEE S. *et al.*, *New J. Phys.*, **15** (2013) 123031.
- [8] ZHOU N., XU X.-F., WANG J.-R., YANG J.-H., LI Y.-K., GUO Y., YANG W.-Z., NIU C.-Q., CHEN B., CAO C. and DAI J.-H., *Phys. Rev. B*, **90** (2014) 094520.
- [9] ZHANG Q.-R., RHODES D., ZENG B., BESARA T., SIEGRIST T., JOHANNES M. D. and BALICAS L., *Phys. Rev. B*, **88** (2013) 024508.
- [10] CARRINGTON A. and COOPER J. R., *Physica C*, **219** (1994) 119.
- [11] CARRINGTON A., MACKENZIE A. P., LIN C. T. and COOPER J. R., *Phys. Rev. Lett.*, **69** (1992) 2855.
- [12] SÉNÉCHAL D., LAVERTU P.-L., MAROIS M.-A. and TREMBLAY A.-M., *Phys. Rev. Lett.*, **94** (2005) 156404.
- [13] DE LA CRUZ C., HUANG Q., LYNN J., LI J., RATCLIFF II W., ZARESTKY J. L., MOOK H., CHEN G., LUO J., WANG N. *et al.*, *Nature*, **453** (2008) 899.
- [14] CAVIGLIA A. D., GABAY M., GARIGLIO S., REYREN N., CANCELLIERI C. and TRISONE J.-M., *Phys. Rev. Lett.*, **104** (2010) 126803.
- [15] GARDNER H. J., KUMAR A., YU L., XIONG P., WARUSAWITHANA M. P., WANG L., VAFEK O. and SCHLOM D. G., *Nat. Phys.*, **7** (2011) 895.
- [16] SHAO D., LUO X., LU W., HU L., ZHU X., SONG W., ZHU X. and SUN Y., *arXiv preprint arXiv:1510.05719*, (2015) .
- [17] LEE P. A., NAGAOSA N. and WEN X.-G., *Rev. Mod. Phys.*, **78** (2006) 17.
- [18] STEWART G. R., *Rev. Mod. Phys.*, **83** (2011) 1589.
- [19] VAKNIN D., SINHA S. K., MONCTON D. E., JOHNSTON D. C., NEWSAM J. M., SAFINYA C. R. and KING H. E., *Phys. Rev. Lett.*, **58** (1987) 2802.
- [20] HUANG Q., QIU Y., BAO W., GREEN M. A., LYNN J. W., GASPAREVIC Y. C., WU T., WU G. and CHEN X. H., *Phys. Rev. Lett.*, **101** (2008) 257003.